GUARANTEEING DYNAMIC PERFORMANCE IN NONLINEAR NON-SMOOTH POWER SYSTEMS

Vaibhav Donde * **Ian A. Hiskens** **

* *Department of Electrical and Computer Engineering*
University of Illinois at Urbana-Champaign
Urbana, IL 61801, USA
** *Department of Electrical and Computer Engineering*
University of Wisconsin-Madison
Madison, WI 53706, USA

Abstract: Performance specifications place restrictions on the dynamic response of many systems, including power systems. It is often convenient to know parameter values that induce limiting behaviour, i.e., force the system to just meet the specification. This limiting behaviour is a form of grazing bifurcation, and can be formulated as a boundary value problem. The paper develops a numerical shooting method for computing such bifurcation parameter values, and an optimization algorithm for finding bifurcation values that are closest to a given parameter set.

Keywords: Nonlinear system dynamics, grazing bifurcations, shooting methods.

1. INTRODUCTION

Power system dynamic behaviour is generally subject to performance constraints that ensure appropriate post-fault response. Controls on generators and FACTS devices, for example, seek to minimize voltage and/or current excursions. Otherwise excessive swings may trigger generator or feeder protection, outaging those items of equipment, and possibly leading to cascading system failure. Bounding cases, where the system trajectory just (tangentially) encounters a performance constraint, separate regions of desirable and undesirable behaviour. Figure 1 provides an illustration.

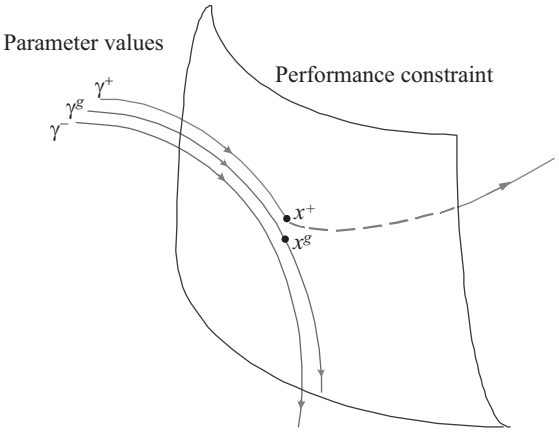

Fig. 1. Grazing phenomenon.

Referring to Figure 1, for a certain value of parameter γ^+, the system trajectory encounters a performance constraint at a point x^+. An event possibly occurs, and the trajectory continues accordingly. However for a small change in parameter value, to γ^-, the trajectory misses (at least locally) the constraint, and subsequently exhibits a completely different form of response. At a parameter value γ^g, lying between γ^+ and γ^-, the trajectory tangentially encounters (*grazes*) the

⋆ Research supported by the National Science Foundation through grant ECS-0332777.

constraint. Behaviour beyond the grazing point x^g is generally unpredictable, in the sense that without further knowledge of the system, it is impossible to determine whether or not an event triggers. This bounding case describes a *grazing bifurcation*, see (di Bernardo *et al.*, 2001) for example, with γ^g referring to the critical value of the bifurcation parameter.

Vulnerability to event triggering can be assessed by comparing given (nominal) parameter values with values that induce grazing. If a sufficient margin exists between actual and grazing values, then dynamic performance is guaranteed. Crucial to this assessment is the ability to determine grazing values. A shooting method was developed in (Donde and Hiskens, 2003) for locating grazing bifurcations. However *a priori* knowledge of the parameter space search direction was required. This paper generalizes that earlier formulation, by developing an algorithm that searches over parameter space for the closest grazing bifurcation. The resulting distance provides a more complete indication of robustness to grazing.

2. HYBRID SYSTEM MODEL

Power systems exhibit hybrid system behaviour, which is characterized by continuous and discrete states, continuous dynamics, discrete events (triggers), and mappings that define the evolution of discrete states at events. It is shown in (Hiskens, 2004) that such behaviour can be captured by a model which consists of a set of differential-algebraic equations, adapted to incorporate impulsive (state reset) action and switching of the algebraic equations. This *DA Impulsive Switched* (DAIS) model can be written in the form,

$$\dot{x} = f(x,y) + \sum_{j=1}^{r} \delta(y_{r[j]}) \Big(h_j(x,y) - x \Big) \qquad (1)$$

$$0 = g(x,y) \equiv g^{(0)}(x,y) + \sum_{i=1}^{s} g^{(i)}(x,y) \qquad (2)$$

where

$$g^{(i)}(x,y) = \begin{cases} g^{(i-)}(x,y) & y_{s[i]} < 0 \\ g^{(i+)}(x,y) & y_{s[i]} > 0 \end{cases} \quad i = 1,...,s \qquad (3)$$

$x \in \mathbb{R}^n$ are dynamic states, $y \in \mathbb{R}^m$ are algebraic states, and $\delta(.)$ is the Dirac delta. Also $r[j]$ indexes the element of y that triggers the j-th reset event, and $s[i]$ provides the index for the i-th switching event. Full details of the model (1)-(3) can be found in (Hiskens, 2004).

A compact development of the equations describing grazing phenomena results from incorporating parameters $\gamma \in \mathbb{R}^\ell$ into the dynamic states x. (Numerical implementation is also simplified.) This is achieved by introducing trivial differential equations $\dot{\gamma} = 0$ into (1).

Away from events, system dynamics evolve smoothly according to the familiar differential-algebraic model

$$\dot{x} = f(x,y) \qquad (4)$$

$$0 = g(x,y) \qquad (5)$$

where g is composed of $g^{(0)}$ together with appropriate choices of $g^{(i-)}$ or $g^{(i+)}$, depending on the sign of the respective $y_{s[i]}$. The *flows* of x and y are defined as

$$x(t) = \phi_1(x_0, t) \qquad (6)$$

$$y(t) = \phi_2(x_0, t) \qquad (7)$$

where $x(t)$ and $y(t)$ satisfy (1)-(3), along with initial conditions $\phi_1(x_0, t_0) = x_0$.

3. GRAZING BIFURCATIONS

3.1 Formulation

Grazing is characterised by a trajectory (flow) of the system touching a target hypersurface tangentially. Let that hypersurface be described by

$$b(x,y) = 0 \qquad (8)$$

where $b : \mathbb{R}^{n+m} \to \mathbb{R}$. Tangency of the flow corresponds to $[\dot{x}^T \ \dot{y}^T]\nabla b = b_x f(x,y) + b_y v = 0$, where $v \equiv \dot{y}$. A single degree of freedom is available for varying parameters to find a grazing point. Recall that parameters γ are incorporated into the initial conditions x_0. Therefore the single degree of freedom can be achieved by parameterization $x_0(\theta)$, where θ is a scalar.

It is shown in (Donde and Hiskens, 2003) that grazing points are described by combining together the flow definition (6) (appropriately parameterized by θ), algebraic equations (5), target hypersurface (8), and tangency conditions to give

$$F_{g1}(x_g, \theta, t_g) := \phi_1(x_0(\theta), t_g) - x_g = 0 \qquad (9)$$

$$F_{g2}(x_g, y_g) := g(x_g, y_g) = 0 \qquad (10)$$

$$F_{g3}(x_g, y_g) := b(x_g, y_g) = 0 \qquad (11)$$

$$F_{g4}(x_g, y_g, v) := \begin{bmatrix} b_x & b_y \\ g_x & g_y \end{bmatrix} \begin{bmatrix} f(x_g, y_g) \\ v \end{bmatrix} = 0 \qquad (12)$$

where the partial derivatives in (12) are evaluated at the grazing point x_g, y_g. Grazing occurs at time t_g along the trajectory. This set of equations may be written compactly as

$$F_g(x_g, y_g, \theta, t_g, v) = F_g(z) = 0 \qquad (13)$$

where $F_g : \mathbb{R}^{n+2m+2} \to \mathbb{R}^{n+2m+2}$ and $z = [x_g^T \ y_g^T \ \theta \ t_g \ v^T]^T$.

3.2 Shooting method

Numerical solution of (13) using Newton's method amounts to iterating on the standard update formula

$$z^{k+1} = z^k - \left(DF_g(z^k)\right)^{-1} F_g(z^k) \qquad (14)$$

where DF_g is the Jacobian matrix

$$DF_g = \begin{bmatrix} -I & 0 & \Phi_1 \dfrac{dx_0}{d\theta} & f & 0 \\ g_x & g_y & 0 & 0 & 0 \\ b_x & b_y & 0 & 0 & 0 \\ f^T b_{xx} + b_x f_x + v^T b_{yx} & f^T b_{xy} + b_x f_y + v^T b_{yy} & 0 & 0 & b_y \\ \hat{f}^T g_{xx} + g_x f_x + \hat{v}^T g_{yx} & \hat{f}^T g_{xy} + g_x f_y + \hat{v}^T g_{yy} & 0 & 0 & g_y \end{bmatrix} \qquad (15)$$

with

$$\hat{f} = \begin{bmatrix} f & & & \\ & f & & \\ & & f & \\ & & & \ddots \\ & & & & f \end{bmatrix}, \; \hat{v} = \begin{bmatrix} v & & & \\ & v & & \\ & & v & \\ & & & \ddots \\ & & & & v \end{bmatrix} \qquad (16)$$

$$g_{xx} = \begin{bmatrix} \dfrac{\partial^2 g_1}{\partial x^2} \\ \dfrac{\partial^2 g_2}{\partial x^2} \\ \vdots \\ \dfrac{\partial^2 g_m}{\partial x^2} \end{bmatrix}, \qquad g_{yx} = \begin{bmatrix} \dfrac{\partial^2 g_1}{\partial y \partial x} \\ \dfrac{\partial^2 g_2}{\partial y \partial x} \\ \vdots \\ \dfrac{\partial^2 g_m}{\partial y \partial x} \end{bmatrix} \qquad (17)$$

$$g_{yy} = \begin{bmatrix} \dfrac{\partial^2 g_1}{\partial y^2} \\ \dfrac{\partial^2 g_2}{\partial y^2} \\ \vdots \\ \dfrac{\partial^2 g_m}{\partial y^2} \end{bmatrix}, \qquad g_{xy} = \begin{bmatrix} \dfrac{\partial^2 g_1}{\partial x \partial y} \\ \dfrac{\partial^2 g_2}{\partial x \partial y} \\ \vdots \\ \dfrac{\partial^2 g_m}{\partial x \partial y} \end{bmatrix}. \qquad (18)$$

The matrices g_{xx}, g_{yx}, g_{xy} and g_{yy} are usually extremely sparse. They can be obtained by numerical differencing. However by utilizing an object oriented modelling structure, these second derivative terms occur only within components. There are no terms introduced by inter-component dependencies. Explicit formulae for these second derivatives can be established for each component model. The sparse matrices can then be efficiently constructed.

The entry Φ_1 in (15) gives the sensitivity of the flow (6) to perturbations in initial conditions x_0,

$$\Phi_1(t) \equiv \frac{\partial \phi_1}{\partial x_0}(x_0, t).$$

The variational equations describing the evolution of trajectory sensitivities Φ_1, Φ_2 are given in (Hiskens and Pai, 2000). These quantities are defined for non-smooth trajectories generated by hybrid systems, and can be efficiently computed as a by-product of implicit integration.

4. CLOSEST BIFURCATIONS

Isolated grazing bifurcation points require a single degree of freedom in parameter space i.e., $\theta \in \mathbb{R}$. However in practice system response is affected by many parameters. If multiple parameters are allowed to vary, a continuum of bifurcation points is obtained. Bifurcations therefore define a hypersurface Σ in parameter space.

Assume that parameter space has dimension p. Nominal (initial) parameter values correspond to a point $\theta_0 \in \mathbb{R}^p$. The distance between θ_0 and the grazing bifurcation hypersurface $\Sigma \subset \mathbb{R}^p$ provides an indication of the robustness of the system to grazing phenomena. A small distance would suggest that the system was vulnerable to grazing. Therefore identifying points on Σ that are (locally) closest to θ_0 is important in many application areas, including power systems. The direction from θ_0 to those closest points describes the "worst case" for parameter variations.

Locally closest points on Σ are called *closest bifurcations* (Dobson, 2003). An analytical description of such points is formulated in the following section. Their computation is discussed in Section 4.2.

4.1 Mathematical formulation

Initially consider the optimization problem [1]

$$\min ||\theta - \theta_0||_2^2 \qquad (19)$$

$$\text{s.t. } F(\theta) = 0 \qquad (20)$$

where grazing bifurcations are given by $F(\theta) = 0$, that is $\Sigma = \{\theta : F(\theta) = 0\}$, and $F : \mathbb{R}^p \to \mathbb{R}^l$. The corresponding Lagrangian is given by

$$\mathcal{L}(\theta, \lambda) = ||\theta - \theta_0||_2^2 + \lambda^T F(\theta) \qquad (21)$$

and the optimal solution by

$$\nabla \mathcal{L}(\theta, \lambda) = \begin{bmatrix} 2(\theta - \theta_0) + \dfrac{\partial F}{\partial \theta}^T \lambda \\ F(\theta) \end{bmatrix} = 0. \qquad (22)$$

The optimal solution lies on the $(p-l)$-manifold $F(\theta) = 0$, at a point where $(\theta - \theta_0)$ is a linear combination of ∇F_1, ∇F_2, $\cdots$, ∇F_l. In other words, $(\theta - \theta_0)$ lies in the hyperplane spanned

[1] The Euclidean norm is used throughout this paper. Similar developments apply for other norms.

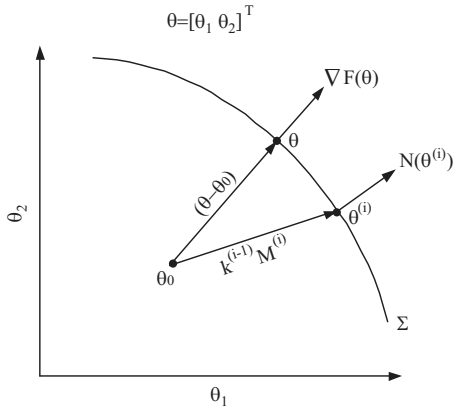

Fig. 2. Geometry of closest bifurcations.

by the gradient vectors. Figure 2 illustrates the geometry of this optimization problem for $p = 2$ and $l = 1$. Note that at the closest bifurcation point, $(\theta - \theta_0)$ aligns with the gradient vector $\nabla F(\theta)$, which defines the normal $N(\theta)$ to Σ at θ. Other aspects of Figure 2 are discussed in Section 4.2.

Referring back to (13), it can be seen that the grazing bifurcation description does not have exactly the form of (20). A more general optimization formulation is required,

$$\min ||\theta - \theta_0||_2^2 \tag{23}$$
$$\text{s.t. } F_g(\theta, \tilde{z}) = 0 \tag{24}$$

where $\tilde{z} = [x_g^T \ y_g^T \ t_g \ v^T]^T \in \mathbb{R}^{n+2m+1}$, $\theta \in \mathbb{R}^p$, and $F_g : \mathbb{R}^{n+2m+1+p} \rightarrow \mathbb{R}^{n+2m+2}$. If $p = 1$, so that θ is a scalar parameter, then (24) defines 0-manifolds, or point solutions. There are no degrees of freedom to optimize over. This is the standard grazing bifurcation problem discussed in Section 3.

If $p > 1$, the Lagrangian becomes

$$\mathcal{L}(\theta, \tilde{z}, \lambda) = ||\theta - \theta_0||_2^2 + \lambda^T F_g(\theta, \tilde{z}) \tag{25}$$

and optimal solutions are given by

$$\nabla\mathcal{L}(\theta, \tilde{z}, \lambda) = \begin{bmatrix} 2(\theta - \theta_0) + \dfrac{\partial F_g}{\partial \theta}^T \lambda \\ \dfrac{\partial F_g}{\partial \tilde{z}}^T \lambda \\ F_g(\theta, \tilde{z}) \end{bmatrix} = 0. \tag{26}$$

Well defined solutions require $\text{rank}\{\frac{\partial F_g}{\partial \tilde{z}}\} = n + 2m + 1$.

To establish a connection between (26) and (22), it is convenient to form the partition

$$\frac{\partial F_g}{\partial \tilde{z}} = \overset{n+2m+1}{\begin{bmatrix} F_{z1} \\ \cdots \\ F_{z2} \end{bmatrix}} \begin{matrix} n+2m+1 \\ \cdots \\ 1 \end{matrix} \tag{27}$$

where the dimensions of the submatrices F_{z1} and F_{z2} are indicated. (The above rank condition ensures that a nonsingular F_{z1} exists.) Correspondingly,

$$\frac{\partial F_g}{\partial \theta} = \overset{p}{\begin{bmatrix} F_{\theta 1} \\ \cdots \\ F_{\theta 2} \end{bmatrix}} \begin{matrix} n+2m+1 \\ \cdots \\ 1 \end{matrix} \tag{28}$$

$$\lambda = \overset{1}{\begin{bmatrix} \lambda_1 \\ \cdots \\ \lambda_2 \end{bmatrix}} \begin{matrix} n+2m+1 \\ \cdots \\ 1 \end{matrix} \tag{29}$$

The first two equations of (26) can then be rewritten,

$$\begin{bmatrix} F_{\theta 1}^T & F_{\theta 2}^T \\ F_{z1}^T & F_{z2}^T \end{bmatrix} \begin{bmatrix} \lambda_1 \\ \lambda_2 \end{bmatrix} = \begin{bmatrix} -2(\theta - \theta_0) \\ 0 \end{bmatrix}. \tag{30}$$

Given that F_{z1} is nonsingular, (30) can be reduced to

$$2(\theta - \theta_0) + \underbrace{(F_{\theta 2}^T - F_{\theta 1}^T F_{z1}^{-T} F_{z2}^T)}_{\tilde{F}_\theta^T} \lambda_2 = 0. \tag{31}$$

From (26) and (31), optimal solutions are given by,

$$\nabla\mathcal{L}(\theta, \tilde{z}, \lambda) = \begin{bmatrix} 2(\theta - \theta_0) + \tilde{F}_\theta^T \lambda_2 \\ F_g(\theta, \tilde{z}) \end{bmatrix} = 0. \tag{32}$$

Notice that (32) is directly comparable with (22), with the optimal point lying on the manifold $F_g(\theta, \tilde{z}) = 0$ at the location where the vector $(\theta - \theta_0)$ aligns with the vector $N(\theta) = \tilde{F}_\theta^T$ that is normal to Σ at θ.

The matrix $\frac{\partial F_g}{\partial \tilde{z}}$ is constructed from DF_g in (15) by removing the third block column. That column becomes $\frac{\partial F_g}{\partial \theta}$. Rather than obtaining $\tilde{F}_\theta$ as in (31), it is computationally more efficient to solve the middle equation of (26) for λ using a Gaussian elimination process, and substitute into the first equation of (26).

4.2 Iterative method for closest bifurcation

The iterative method utilizes the fact that vectors $(\theta - \theta_0)$ and $N(\theta)$ align at the closest bifurcation point. This method is adapted from (Dobson, 2003). It converges locally to closest bifurcations if Σ is convex (at least locally) or if it is only slightly concave.

Referring to Figure 2, let k be a unit vector in $\mathbb{R}^p$ defining the direction of parameter change from θ_0. As parameters vary along k from θ_0, the grazing bifurcation hypersurface Σ will be encountered. The shooting method (14) can be used to locate that intersection point. Let M be the distance from θ_0 to the grazing point along k, or equivalently $||\theta - \theta_0||_2$. The following iterative procedure seeks to minimize M.

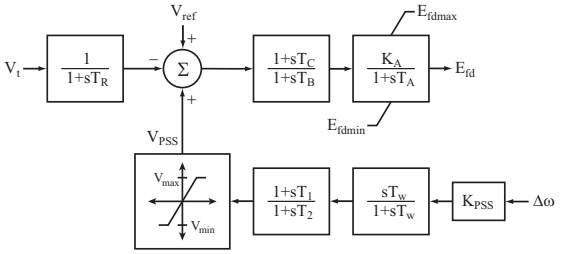

Fig. 3. Excitation system (AVR/PSS) representation.

(1) Let $k^{(0)}$ be an initial guess for k. For example, this initialization can be achieved by freeing a single parameter and holding other parameters fixed.
(2) Given $k^{(i-1)}$, compute the first grazing point in the direction $k^{(i-1)}$; that is, compute $M^{(i)}$ and $\theta^{(i)}$ so that $\theta^{(i)} = \theta_0 + k^{(i-1)}M^{(i)} \in \Sigma$.
(3) Compute the vector $N(\theta^{(i)})$ normal to Σ at $\theta^{(i)}$. Figure 2 illustrates the computation of $\theta^{(i)}$ and $N(\theta^{(i)})$ graphically.
(4) Set $k^{(i)} = N(\theta^{(i)})$. Iterate until convergence of $k^{(i)}$ to k^*. The (locally) closest bifurcation point occurs at $\theta^* = \theta_0 + k^*M^*$.

The direction k^* of a closest bifurcation is aligned with the normal vector $N(\theta^*)$, and is the fixed point of the iterations. Note that in the special case of Σ being a hyperplane, iterations converge in one step.

5. EXAMPLE

A single machine infinite bus power system will be used for illustrations. The generator was accurately represented by a sixth order machine model (Sauer and Pai, 1998), and the generator excitation system was modelled according to Figure 3. Note that the output limits on the field voltage E_{fd} are anti-wind-up limits, while the limits on the stabilizer output V_{PSS} are clipping limits. Therefore even though this example utilizes a simple network structure, it exhibits nonlinear, non-smooth, hybrid system behaviour. Larger systems are no more challenging. A single phase fault was applied at the generator terminal bus at 0.05 sec. The fault was cleared, without line tripping, at 0.28 sec.

Generators are susceptible to over-voltage protection operation if their terminal voltage rises too high. This may occur during transients following a large disturbance. The field voltage maximum limit E_{fdmax}, and PSS output limits V_{max} and V_{min}, have a large influence on transient over-voltages. Therefore this example considers values of those parameters that ensure the initial terminal voltage overshoot does not rise above a specified value of 1.2 pu. The target hypersurface in this example is therefore $V_t - 1.2 = 0$.

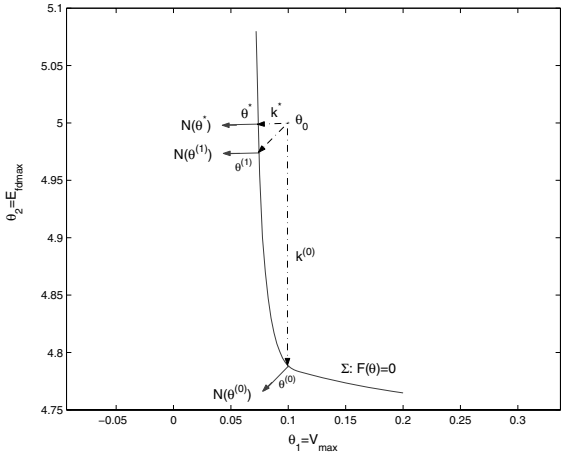

Fig. 4. Convergence in parameter space, $\theta = [V_{max}\ E_{fdmax}]^T$.

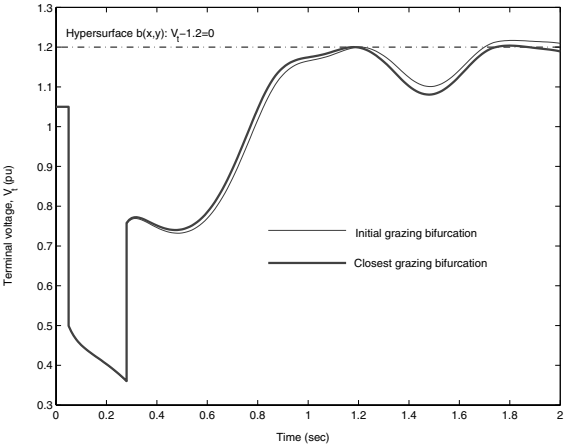

Fig. 5. Terminal voltage, V_t.

Initially consider V_{max} and E_{fdmax} as free parameters, so that $\theta = [V_{max}\ E_{fdmax}]^T$. Convergence to the closest bifurcation point occurred in three iterations. The iterative process is presented graphically in Figure 4, and tabulated in Table 1. Figure 5 shows the time domain response of terminal voltage V_t. The initial grazing bifurcation, corresponding to $\theta^{(0)}$ is shown in the figure, along with the grazing bifurcation for the closest parameter set θ^*. Notice that in both cases the trajectory is tangential to the target hypersurface.

Figure 4 indicates that the bifurcation hypersurface Σ is quite nonlinear, with a sharp turning point near $\theta = [0.1\ 4.7575]^T$. The initial point $\theta^{(0)}$ was obtained with $k^{(0)} = [0\ 1]^T$, i.e., variation of E_{fdmax} only. Even though this was a poor choice, with $\theta^{(0)}$ some distance from θ^*, convergence was reliable due to the local convexity of Σ.

Consider now the case where all three parameters are free to vary simultaneously. The hypersurface Σ becomes a surface in $\mathbb{R}^3$. Figure 6 shows a view of slices of Σ, where the surface is cut parallel to the V_{max}-E_{fdmax} plane. These equi-V_{min} curves were produced using a continuation method. The

Iteration	V_{max}	E_{fdmax}	k^T
0	0.1000	4.7880	[0.0000 1.0000]
1	0.0745	4.9739	[-0.6980 -0.7153]
2	0.0739	4.9994	[-0.9997 -0.0244]
3	0.0739	4.9994	[-0.9997 -0.0242]

Table 1. Convergence progress, two free parameters.

Iter	$[V_{max}\ V_{min}\ E_{fdmax}]$	k^T
0	0.1000 -0.1000 4.7883	0.0000 0.0000 1.0000
1	0.0879 -0.1218 4.9877	-0.4325 -0.7854 -0.4428
2	0.0815 -0.1120 4.9996	-0.8401 -0.5422 -0.0167
3	0.0814 -0.1119 4.9996	-0.8432 -0.5372 -0.0183
4	0.0815 -0.1119 4.9996	-0.8433 -0.5371 -0.0183

Table 2. Convergence progress, three free parameters.

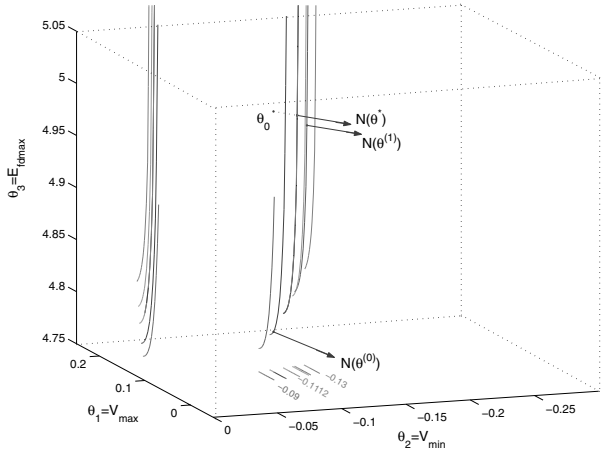

Fig. 6. Convergence in parameter space, $\theta = [V_{max}\ V_{min}\ E_{fdmax}]^T$.

figure also shows the projection of these curves on the V_{max}-E_{fdmax} and V_{max}-V_{min} planes. Note that the projection on the V_{max}-E_{fdmax} plane corresponds to Figure 4, drawn for various values of V_{min}. The projections of the equi-V_{min} curves on the V_{max}-V_{min} plane are straight lines parallel to the V_{max} axis. The corresponding values of V_{min} are noted in the figure.

Results of the iterative process are given in Table 2. Reliable convergence was obtained in 4 iterations, even though the initial guess of $k^{(0)} = [0\ 0\ 1]^T$ was quite poor. The vector $(\theta^* - \theta^{(0)})$ aligns with the normal $N(\theta^*)$ at convergence.

It is perhaps not evident from Figure 5, but this system exhibits quite non-smooth behaviour. In fact, fifteen events occur over the initial 2 sec transient, primarily V_{PSS} banging on maximum and minimum limits. Discrete events exert a strong influence on system dynamics. However because the Jacobian DF_g takes those events into account, through the trajectory sensitivities Φ_1, shooting method convergence is unaffected.

6. CONCLUSIONS

Performance specifications place restrictions on the dynamic response of systems. These specifications dictate regions of parameter space where operation is acceptable. Parameter values on the boundary of such a region give rise to behaviour that just meets the specification. This situation corresponds to a grazing phenomenon.

The paper formulates grazing conditions as a set of nonlinear, algebraic equations. Iterative solution via Newton's method requires numerical integration of the system trajectory, and therefore has the form of a shooting method. The associated Jacobian incorporates trajectory sensitivities, which can be efficiently computed along with the trajectory. The shooting method is therefore practical for arbitrarily large hybrid systems.

The shooting method searches in a specified direction, in parameter space, for a grazing bifurcation. However for a given parameter set, closer bifurcations may lie in a different direction. The paper has formulated and illustrated an optimization algorithm for locating the (locally) closest grazing bifurcation point. The shooting method is utilized at each iteration of the optimization process.

REFERENCES

di Bernardo, M., C.J. Budd and A.R. Champneys (2001). Grazing and border-collision in piecewise-smooth systems: A unified analytical framework. *Physical Review Letters* **86**(12), 2553–2556.

Dobson, I. (2003). Distance to bifurcation in multidimensional parameter space: Margin sensitivity and closest bifurcations. In: *Bifurcation Control, Theory and Application*. G. Chen, D.J. Hill and X. Yu (Editors), Lecture Notes in Control and Information Sciences, Vol. 293, Springer-Verlag, New York.

Donde, V. and I.A. Hiskens (2003). Shooting for border collision bifurcations in hybrid systems. In: *Proceedings of the 42nd IEEE Conference on Decision and Control*. Maui, HI.

Hiskens, I.A. (2004). Power system modeling for inverse problems. *IEEE Transactions on Circuits and Systems I: Regular Papers* **51**(3), 539–551.

Hiskens, I.A. and M.A. Pai (2000). Trajectory sensitivity analysis of hybrid systems. *IEEE Transactions on Circuits and Systems I* **47**(2), 204–220.

Sauer, P.W. and M.A. Pai (1998). *Power System Dynamics and Stability*. Prentice Hall. Upper Saddle River, NJ.